AGU PUBLICATIONS

Geophysical Research Letters

RESEARCH LETTER
10.1002/2016GL067765

Key Points:
- Horizontal water vapor transport has higher predictability than precipitation in the western U.S.
- Water vapor transport and precipitation exhibit large variation in winter-to-winter predictability
- Small ensemble spreads have initiation states with high geopotential heights south of Alaska

Correspondence to:
D. A. Lavers,
david.lavers@ecmwf.int

Citation:
Lavers, D. A., D. E. Waliser, F. M. Ralph, and M. D. Dettinger (2016), Predictability of horizontal water vapor transport relative to precipitation: Enhancing situational awareness for forecasting western U.S. extreme precipitation and flooding, *Geophys. Res. Lett.*, *43*, doi:10.1002/2016GL067765.

Received 12 JAN 2016
Accepted 17 FEB 2016
Accepted article online 20 FEB 2016

Predictability of horizontal water vapor transport relative to precipitation: Enhancing situational awareness for forecasting western U.S. extreme precipitation and flooding

David A. Lavers[1,2], Duane E. Waliser[1,3], F. Martin Ralph[1], and Michael D. Dettinger[1,4]

[1]Center for Western Weather and Water Extremes, Scripps Institution of Oceanography, University of California, San Diego, La Jolla, California, USA, [2]Now at European Centre for Medium-Range Weather Forecasts, Reading, UK, [3]Jet Propulsion Laboratory, California Institute of Technology, Pasadena, California, USA, [4]U.S. Geological Survey, Carson City, Nevada, USA

Abstract The western United States is vulnerable to socioeconomic disruption due to extreme winter precipitation and floods. Traditionally, forecasts of precipitation and river discharge provide the basis for preparations. Herein we show that earlier event awareness may be possible through use of horizontal water vapor transport (integrated vapor transport (IVT)) forecasts. Applying the potential predictability concept to the National Centers for Environmental Prediction global ensemble reforecasts, across 31 winters, IVT is found to be more predictable than precipitation. IVT ensemble forecasts with the smallest spreads (least forecast uncertainty) are associated with initiation states with anomalously high geopotential heights south of Alaska, a setup conducive for anticyclonic conditions and weak IVT into the western United States. IVT ensemble forecasts with the greatest spreads (most forecast uncertainty) have initiation states with anomalously low geopotential heights south of Alaska and correspond to atmospheric rivers. The greater IVT predictability could provide warnings of impending storminess with additional lead times for hydrometeorological applications.

1. Introduction

Extreme hydrometeorological events, or heavy precipitation and floods, have large adverse socioeconomic consequences. Medium-range precipitation forecasts from numerical weather prediction models and river flow forecasts from hydrological models are now used as key inputs for warnings for such events, providing information on when particular locations are most at risk, allowing for measures to mitigate potential damages. The level of situational awareness (such as is needed by people in the emergency preparedness community) depends largely on the predictability of the extreme event, where the predictability is an inherent property of the event; this is in contrast to the predictive skill, which quantifies the capability of a forecast system. As different variables (e.g., precipitation and river discharge) have varying levels of predictability, it follows that the predictability, and thus awareness of extreme events, also varies depending on the variable monitored to anticipate such events.

In many midlatitude locations, most of the largest precipitation and flood events, especially in coastal regions, are related to intense vertically integrated horizontal water vapor transport (integrated vapor transport, IVT) approaching within extratropical cyclones, in regions known as atmospheric rivers (ARs) [e.g., *Zhu and Newell*, 1998; *Ralph et al*., 2006, 2013; *Lavers et al*., 2011; *Neiman et al*., 2011]. As the AR region (and hence IVT) is closely associated with extratropical cyclones, ARs are generally related to large-scale (or synoptic-scale) atmospheric processes. Conversely, precipitation amounts generally reflect highly localized processes, with smaller-scale (or mesoscale) atmospheric processes, such as frontal convergence and complex land-atmosphere interactions, affecting precipitation variability. As a consequence of these scale differences, precipitation is likely to be less predictable than IVT. Given the strong connection between IVT and precipitation and the differing predictabilities associated with them, *Lavers et al*. [2014] tested the hypothesis that Atlantic ARs, and specifically IVT, would be more predictable than precipitation due to its relationship with the more predictable large-scale circulation. Using the potential predictability methodology (a technique in which the model and real worlds are considered to be identical) on ensemble forecasts from the European Centre for Medium-Range Weather Forecasts (ECMWF) for winter 2013/2014 across Europe, results confirmed that the IVT had higher predictability, with the breakdown in precipitation predictability at shorter lead times mostly explained by errors in the moisture flux convergence. Moreover, an example

was given where the higher IVT predictability could have yielded increased situational awareness of an extreme hydrological event, illustrating the potential to use IVT to extend medium-range warnings of such events.

These findings across Europe raise research questions that this study aims to address. Most immediately, do the IVT and precipitation predictability comparisons over Europe in winter also apply in another region, namely, the eastern North Pacific Ocean and western United States? This region is affected by ARs in the winter, a time when ARs provide a large proportion of the water resources (particularly in California) [*Dettinger et al*., 2011] and are a major cause of flooding [e.g., *Ralph et al*., 2006]. In this paper, we evaluate the findings across Europe for the Pacific-North American sector and extend the reach of those earlier findings. In particular, in this paper, we investigate whether predictability exhibits interannual (winter-to-winter) variability, as well as whether certain initial large-scale atmospheric conditions (or background flows) yield forecasts with the least and greatest ensemble spreads and thus uncertainties? Answers to these questions —including quantification of the rate of decline of predictability with lead time—are of importance to organizations responsible for preparing for extremes. To address these questions, we evaluate the IVT and precipitation reforecasts (over forecast days 1–16) from the National Centers for Environmental Prediction (NCEP) Global Ensemble Forecast System (GEFS) [*Hamill et al*., 2013]. We use the NCEP GEFS as opposed to the ECMWF ensemble prediction system because the NCEP GEFS has a long reforecast data set available, which being free of any model upgrades, allows for the interannual variability to be more accurately assessed.

2. Data and Methods

The NCEP GEFS reforecasts were retrieved for each winter (December, January, and February; DJF) day at 00UTC from 1984/1985 to 2014/2015 (31 years; number of reforecasts = 2796) on a regular grid of 1.0° × 1.0° from ftp://ftp.cdc.noaa.gov/Projects/Reforecast2/. The reforecasts are produced using the 2012 model version [*Hamill et al*., 2013] and consist of 1 control member and 10 perturbed ensemble members out to forecast day 16. (Note that the 00UTC 16 January 2015 reforecast is omitted due to incomplete data.) Daily total surface precipitation was calculated at 00UTC. The specific humidity q and the zonal and meridional (u and v, respectively) winds at 300, 500, 700, 850, 925, and 1000 hPa were used at 00UTC and 12UTC throughout the 16 day forecast horizon to determine daily averaged (using 00UTC, 12UTC, and 00UTC of the next day) zonal and meridional IVTs [e.g., *Neiman et al*., 2008]. These daily zonal and meridional components were then combined into the total water vapor transport (IVT). We note that although IVT is a vector, the focus herein is on the IVT magnitude. Hereafter, we use the term forecast as a synonym for reforecast.

We employ the potential predictability methodology [e.g., *Waliser et al*., 2003; *Luo and Wood*, 2006; *Kumar et al*., 2014] to compare the predictabilities of precipitation and IVT forecasts. This approach assumes that each ensemble member can be used as a surrogate observed realization. Although this assumption is not strictly true, it has been found to be a useful technique for estimating predictability of phenomena using models [e.g., *Palmer*, 2005; *Neena et al*., 2014; *Waliser*, 2011] and has the benefit of being free of the spatiotemporal heterogeneities of the observing network [*Lavers et al*., 2014]. In this framework, on a particular forecast day, one ensemble member is treated as an observation, while the average of the other members represents a forecast; this results in two time series relating to each day in the winter seasons. The skill of this forecast is then determined by the coefficient of determination (r^2) or the square of the linear Pearson correlation coefficient r between the two time series. (A square root transformation was applied to the precipitation time series so that they more closely followed a Gaussian distribution.) This procedure is repeated 11 times, each time with a different ensemble member being treated as the observation (as all members are equally possible), so that 11 r^2 values are obtained. The 11, lead time-dependent, r^2 values are then averaged to estimate potential predictability. Herein, the predictability is assessed across the eastern North Pacific Ocean and western North America at a 1° × 1° scale on different forecast days (1–16 days) in 31 winter seasons.

We also retrieved (from the ECMWF server) the ECMWF ERA-Interim reanalysis [*Dee et al*., 2011] 500 hPa geopotential height at 00UTC (on a Gaussian grid of approximately 0.7° × 0.7°) on all DJF days from 1 January 1979 to 28 February 2015 to evaluate the initial large-scale atmospheric conditions that are associated with the smallest and largest ensemble forecast spreads. On each forecast day of the 2796 forecasts, we calculated the standard deviation of the 11-member ensemble at each grid point across 30°N–50°N, 125°W–120°W and then calculated the domain-average standard deviation. The domain-average standard deviations on each

forecast day were then ranked, and the 140 smallest and largest spreads (comprising the 5th and 95th percentiles) were identified. For these 140 events, the composite mean of the ERA-Interim 500 hPa geopotential height anomalies (calculated with respect to the ERA-Interim reanalysis climatological mean using the 00UTC state on all DJF days from 1 January 1979 to 28 February 2015) were then calculated at the forecast analysis time.

3. Results

3.1. Potential Predictability of Precipitation and Water Vapor Transport

Figures 1a–1d illustrates the potential predictability results at 38°N, 122°W (near San Francisco, California) on forecast days 7 and 10 for winter 2014/2015. In the examples shown, we use ensemble member 11 (perturbed member 10) as the truth, and the mean of members 1–10 (control member and first nine perturbed members) as the predictor. When using member 11 as the truth, forecasts of IVT have higher r^2 values than precipitation (cf. Figures 1a and 1c, with Figures 1b and 1d), as highlighted by the closer relative grouping around the 1:1 line, suggesting a more predictable signal occurs in the IVT forecasts than in precipitation. The final estimates of potential predictability (obtained by averaging 11 r^2 values on each forecast day) in Figure 1e verify that predictability deteriorates with increasing lead time and that in the ensemble as a whole, IVT (black line) exhibits higher predictability than precipitation (grey line). Furthermore, the Welch's t test null hypothesis of equal means between the 11 r^2 values for IVT and precipitation can be rejected at the 95% significance level on 9 of the first 10 forecast days (as shown by the black diamonds in Figure 1e), indicating that the different predictability levels between the variables are significant. Using a threshold r^2 of 0.5 to identify useful predictability, these results show that IVT has this level for approximately 1 day of lead time longer than precipitation. Given the strong observed connections between IVT and precipitation (particularly heavy precipitation [e.g., *Ralph et al*., 2013]), this increased level of predictability has the potential to be used to increase situational awareness of upcoming extreme hydrological events.

The potential predictabilities across the eastern North Pacific Ocean and western North America for forecast day 7 in winter 2014/2015 forecasts are displayed for IVT and precipitation in Figures 2a and 2b, respectively. IVT has higher r^2 values, and thus more predictability, than precipitation, with a plume of high IVT predictability ($r^2 > 0.75$) along a southwest-northeast line toward northern California. The highest precipitation r^2 values occur over northern California, a finding which is likely to be due to the presence of the persistent atmospheric ridge off California and the mountainous terrain there. The presence of orography induces horizontal mass convergence and uplift in a fixed location, which leads to higher predictability than those regions where convergence (and hence precipitation) is caused by other atmospheric processes (e.g., frontal dynamics). In regions without orographic uplift, the breakdown in precipitation predictability at shorter lead times is largely due to uncertainty in the moisture flux convergence [*Lavers et al*., 2014].

In Figures 2c and 2d, potential predictability is shown on forecast day 7 of the winter 2009/2010 forecasts (2010 was a wet water year in the Sierra Nevada, California [*Guan et al*., 2010]). These results indicate that the level and patterns of predictability vary between winter 2009/2010 and 2014/2015, with the highest r^2 values for IVT and precipitation over land occurring in southern California and Baja California, Mexico. To further investigate how the predictability varies with season, we calculate the average r^2 values for the grid points within 30°N–50°N, 125°W–120°W (region bounded by white box in Figure 2b) in each winter season from 1984/1985 to 2014/2015 and present the results for forecast day 7 in Figure 2e. First, in agreement with the results previously shown, the IVT exhibits higher predictability than precipitation in the 31 winter seasons, with IVT having $r^2 > 0.5$ in most winters (except 1984/1985 and 2012/2013). The consistently higher IVT predictability suggests that IVT could possibly be used for hydrological applications to increase situational awareness of extreme events. Second, there is large interannual variability of predictability found throughout the study period, as highlighted for IVT, for example, by an r^2 difference of about 0.2 between the 2012/2013 and 2013/2014 winters.

As the example presented in Figure 1e was for the anomalously dry 2014 season in the western United States, we also calculated the potential predictability using all winter days ($n = 2796$) at 38°N, 122°W (Figure 2f). These results underscore the higher IVT predictability, with the Welch's t test null hypothesis of equal means between the 11 r^2 values for IVT and precipitation being rejected at the 95 % significance level on the first 15 forecast days. Hereafter, we focus on IVT because of its higher predictability.

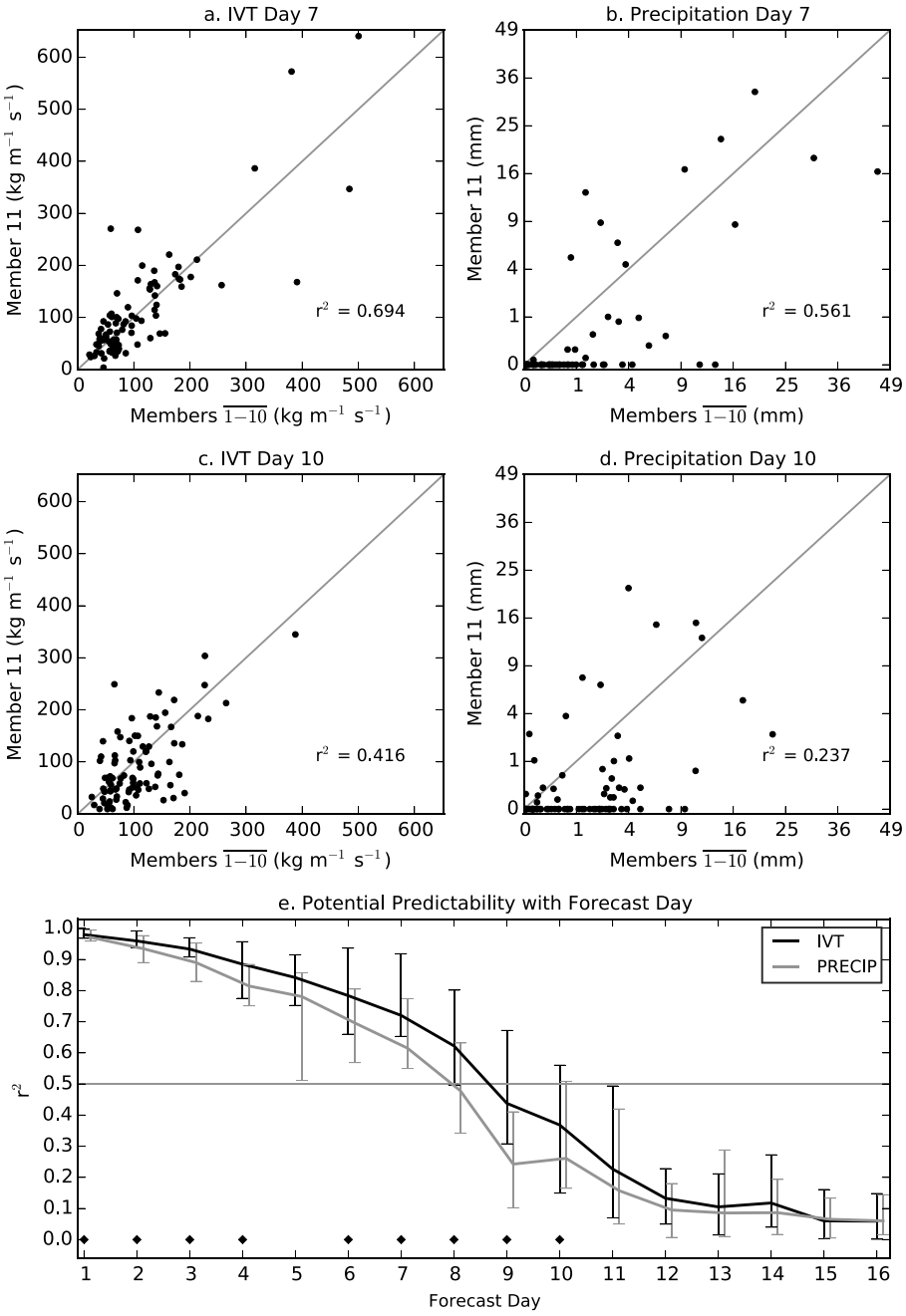

Figure 1. (a–d) An example of the potential predictability approach during winter 2014/2015, where ensemble member 11 is the truth and the average of members 1–10 is the predictor. This is for 38°N, 122°W on forecast day 7 for (a) IVT and (b) precipitation and on forecast day 10 for (c) IVT and (d) precipitation. (e) The predictability throughout the forecast horizon during winter 2014/2015; the error bars are the range of r^2 values; the black diamonds at the bottom show the forecast days when the Welch's unequal variances *t* test null hypothesis of equal means (between IVT and precipitation) can be rejected at the 95% significance level.

3.2. Initial Large-Scale Atmospheric Circulation and IVT Ensemble Spread

This section investigates whether certain initial or analysis states of the large-scale atmospheric circulation give rise to the largest and smallest ensemble spreads and thus uncertainties. Figure 3 shows the composite mean patterns of 500 hPa geopotential height anomalies for large and small IVT ensemble spreads on forecast days 4 and 7.

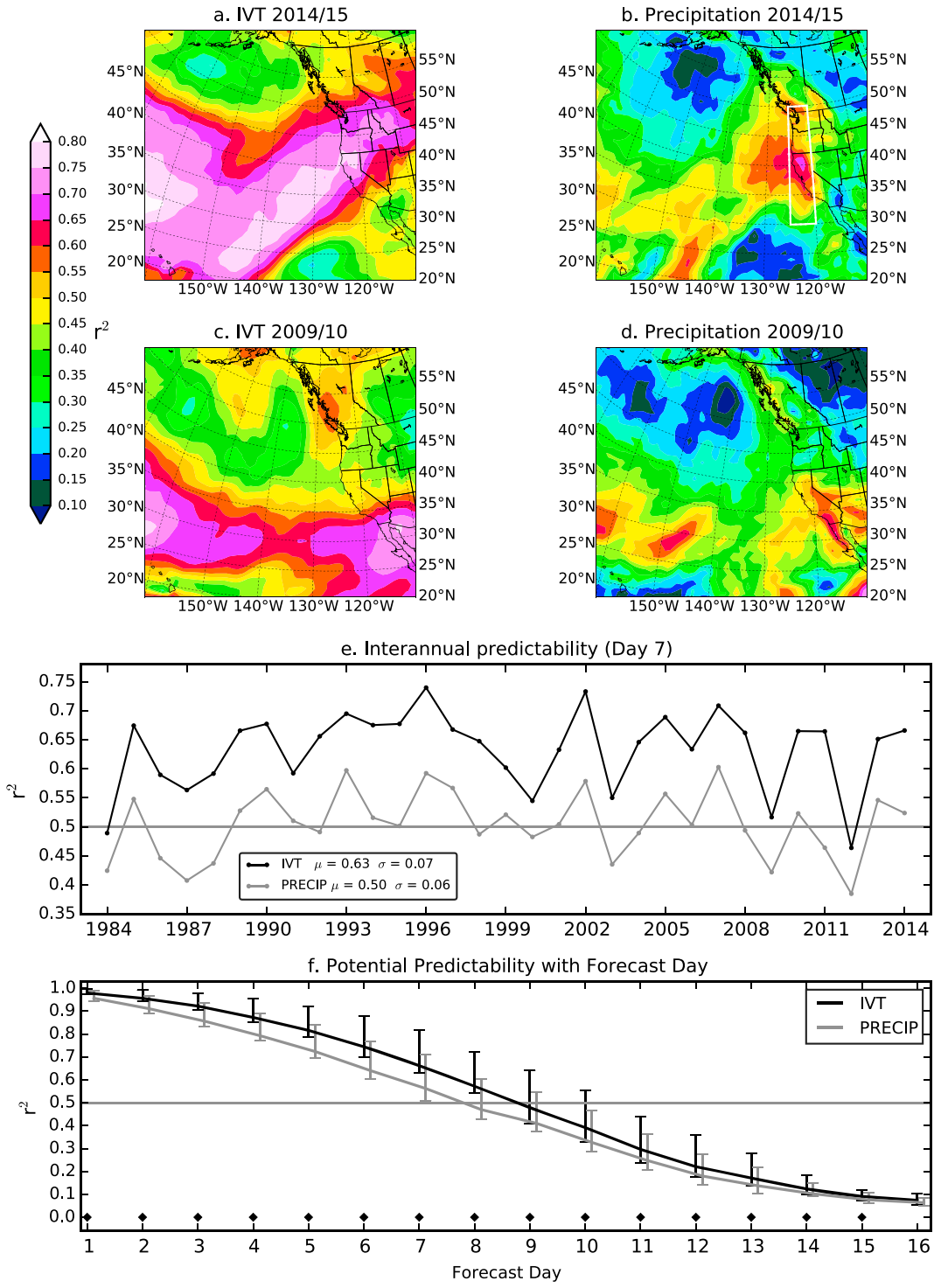

Figure 2. The level of potential predictability (r^2 values) on forecast day 7 for (a, b) 2014/2015 and (c, d) 2009/2010 for IVT and precipitation, respectively. (e) The average interannual predictability (r^2) across the 30°N–50°N, 125°W–120°W region; the domain is shown by the white box in Figure 2b. (f) The predictability throughout the forecast horizon calculated using all winter forecasts ($n = 2796$) at 38°N, 122°W (key as Figure 1e).

On forecast day 4, the forecasts with maximum spread (Figure 3a) have an initial state with below average heights to the south of Alaska and above average heights in a horseshoe shape from Hawaii to the central United States. This setup relates to extratropical cyclone activity off western North America and causes a

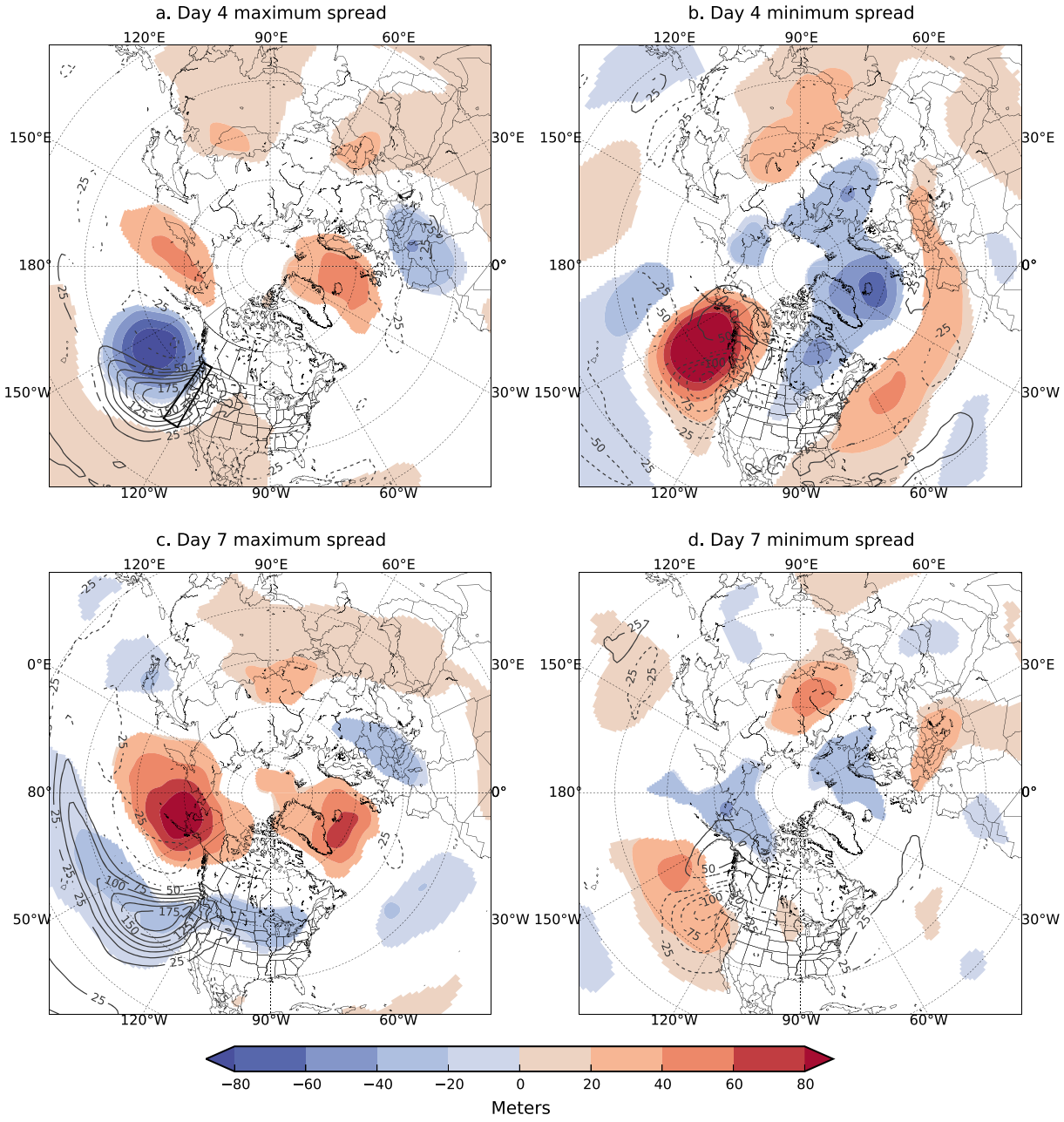

Figure 3. The composite mean of the 500 hPa geopotential height anomalies at the analysis time (shading, in meters) and of the ensemble mean IVT forecast anomalies (contours, dashed where less than climatology; the climatology is determined by averaging the ensemble mean IVT forecasts on all winter days for a particular forecast day) during the 140 largest and smallest ensemble spreads (a and b) on forecast day 4 and (c and d) on forecast day 7. A 90% confidence interval of the mean is calculated at each grid point as $1.645\frac{\sigma}{\sqrt{n}}$, where σ is the standard deviation at each grid of the 140 anomaly fields, and n, the sample size, is 140; colored and contoured regions indicate areas where the composite mean is different from zero at the 90% significance level.

southwesterly flow across the domain, as highlighted by the high anomalous IVT (solid contours in Figure 3a) near the western United States (most likely as atmospheric rivers). During the forecasts with minimum spread (Figure 3b), the composite mean initial forecast state has positive height anomalies to the south of Alaska which occupy a larger region and are stronger than the negative height anomalies found for maximum spread in Figure 3a. This pattern generally leads to low IVT and less variability, as seen by the anomalously low IVT (dashed contours) in Figure 3b. Therefore, these results show that the IVT forecasts are more certain (in terms of forecast spread) when higher than normal geopotential heights are off western North America and more uncertain when lower than normal geopotential heights are present.

For forecasts on day 7 (Figures 3c and 3d), the composites of initial atmospheric states are generally weaker, potentially indicating that a larger range of initial states can lead to the maximum and minimum spreads. For the maximum spreads, a band of negative height anomalies are situated across the eastern North Pacific Ocean and northern contiguous United States suggesting that extratropical cyclones may be developing and propagating through this region, with higher than normal IVT produced (solid contours in Figure 3c) and thus enhanced chances of landfalling atmospheric rivers on the west coast. The high initial heights situated over the Bering Sea may cause cold polar air masses to move off northwestern Canada leading to a strengthening of the temperature gradient and baroclinic zone and hence increase forecast spread and uncertainty across the North Pacific. Conversely, for the minimum spreads, positive height anomalies are centered at about 40°N, 150°W, which leads to a blocked flow pattern, lower than normal IVT (dashed contours in Figure 3d), and more certain forecasts. Moreover, this region of high heights (Figure 3d) is slightly stronger than the low heights in Figure 3c, suggesting that a stronger signal is found for the minimum spread events.

4. Conclusions

The aim of this analysis was to address three research questions: (1) Does the IVT have higher predictability than precipitation across the eastern North Pacific Ocean and western United States? (2) Is there interannual variability in the level of predictability? (3) What forecast analysis states lead to the smallest and largest forecast spread? Using the potential predictability concept, the NCEP GEFS reforecasts for the winters 1984/1985 to 2014/2015 show that IVT does have higher predictability than precipitation. This means that the findings in *Lavers et al*. [2014] on higher IVT predictability across Europe (because of its association with synoptic-scale processes, compared to the more mesoscale processes linked to precipitation) are also applicable across the eastern North Pacific Ocean and western United States. The higher IVT predictability, and the strong connection between IVT and heavy precipitation and floods across the western United States [*Ralph et al*., 2006, 2013; *Neiman et al*., 2011], suggests that IVT may be used to provide earlier situational awareness of extreme hydrological events and the atmospheric rivers behind them. We also found large interannual variability in the predictability levels, with IVT, for example, having an r^2 difference of about 0.2 between the 2012/2013 and 2013/2014 winters. Analysis into the causes of this variability will form future research.

The results show that the forecasts with the smallest ensemble spread and hence uncertainty have an analysis state with anticyclonic conditions off western North America, which leads to reduced extratropical cyclone activity, fewer atmospheric rivers, and thus low water vapor transport into western North America. Evaluation of the largest ensemble spreads shows an analysis state with cyclonic conditions that are more conducive to extreme winter hydrological events, suggesting that extreme event forecasts have most uncertainty. These findings may also provide users a way to assess the forecast ensemble spread in terms of what is expected given the initial state estimate, which has the advantage of potentially affording the identification of possible issues (or unexpected behavior) within the forecast system.

These results support the emerging focus on prediction of landfalling atmospheric rivers, which carry strong IVT and are key to flooding in the western United States and in selected other areas globally.

Acknowledgments
We are grateful for financial support from the California Department of Water Resources. The ERA-Interim data were retrieved from the ECMWF data server. DW's contribution was carried out on behalf of the Jet Propulsion Laboratory, California Institute of Technology, under a contract with NASA. We thank two anonymous reviewers for their comments that helped clarify aspects of the paper.

References

Dee, D. P., et al. (2011), The ERA-Interim reanalysis: Configuration and performance of the data assimilation system, *Q. J. R. Meteorol. Soc.*, *137*(656), 553–597.

Dettinger, M. D., F. M. Ralph, T. Das, P. J. Neiman, and D. Cayan (2011), Atmospheric rivers, floods, and the water resources of California, *Water*, *3*(2), 445–478, doi:10.3390/w3020445.

Guan, B., N. P. Molotch, D. E. Waliser, E. J. Fetzer, and P. J. Neiman (2010), Extreme snow-fall events linked to atmospheric rivers and surface air temperature via satellite measurements, *Geophys. Res. Lett.*, *37*, L20401, doi:10.1029/2010GL044696.

Hamill, T. M., G. T. Bates, J. S. Whitaker, D. R. Murray, M. Fiorino, T. J. Galarneau Jr., Y. Zhu, and W. Lapenta (2013), NOAA's second-generation global medium-range ensemble reforecast dataset, *Bull. Am. Meteorol. Soc.*, *94*, 1553–1565, doi:10.1175/BAMS-D-12-00014.1.

Kumar, A., P. Peng, and M. Chen (2014), Is there a relationship between potential and actual skill? *Mon. Weather Rev.*, *142*, 2220–2227.

Lavers, D. A., R. P. Allan, E. F. Wood, G. Villarini, D. J. Brayshaw, and A. J. Wade (2011), Winter floods in Britain are connected to atmospheric rivers, *Geophys. Res. Lett.*, *38*, L23803, doi:10.1029/2011GL049783.

Lavers, D. A., F. Pappenberger, and E. Zsoter (2014), Extending medium-range predictability of extreme hydrological events in Europe, *Nat. Commun.*, *5*, 5382, doi:10.1038/ncomms6382.

Luo, L., and E. F. Wood (2006), Assessing the idealized predictability of precipitation and temperature in the NCEP Climate Forecast System, *Geophys. Res. Lett.*, *33*, L04708, doi:10.1029/2005GL025292.

Neena, J. M., J. Y. Lee, D. Waliser, B. Wang, and X. Jiang (2014), Predictability of the Madden-Julian oscillation in the Intraseasonal Variability Hindcast Experiment (ISVHE), *J. Clim.*, *27*, 4531–4543.

Neiman, P. J., F. M. Ralph, G. A. Wick, J. D. Lundquist, and M. D. Dettinger (2008), Meteorological characteristics and overland precipitation impacts of atmospheric rivers affecting the West Coast of North America based on eight years of SSM/I satellite observations, *J. Hydrometeorol.*, *9*(1), 22–47.

Neiman, P. J., L. J. Schick, F. M. Ralph, M. Hughes, and G. A. Wick (2011), Flooding in Western Washington: The connection to atmospheric rivers, *J. Hydrometeorol.*, *12*(6), 1337–1358.

Palmer, T. N. (2005), Predictability of weather and climate: From theory to practice, in *Predictability of Weather and Climate*, edited by T. N. Palmer and R. Hagedorn, pp. 1–29, Cambridge Univ. Press, Cambridge, U. K.

Ralph, F. M., P. J. Neiman, G. A. Wick, S. I. Gutman, M. D. Dettinger, D. R. Cayan, and A. B. White (2006), Flooding on California's Russian River: Role of atmospheric rivers, *Geophys. Res. Lett.*, *33*, L13801, doi:10.1029/2006GL026689.

Ralph, F. M., T. Coleman, P. J. Neiman, R. Zamora, and M. D. Dettinger (2013), Observed impacts of duration and seasonality of atmospheric-river landfalls on soil moisture and runoff in coastal northern California, *J. Hydrometeorol.*, *14*, 443–459.

Waliser, D. E. (2011), Predictability and forecasting, in *Intraseasonal Variability of the Atmosphere-Ocean Climate System*, 2nd ed., edited by W. K. M. Lau and D. E. Waliser, 613 pp., Springer, Heidelberg, Germany.

Waliser, D. E., K. M. Lau, W. Stern, and C. Jones (2003), Potential predictability of the Madden-Julian oscillation, *Bull. Am. Meteorol. Soc.*, *84*(1), 33–50.

Zhu, Y., and R. E. Newell (1998), A proposed algorithm for moisture fluxes from atmospheric rivers, *Mon. Weather Rev.*, *126*(3), 725–735, doi:10.1175/1520-0493(1998)126<0725:APAFMF>2.0.CO;2.